SARS-CoV-2 exhibits intra-host genomic plasticity and low-frequency polymorphic quasispecies

Timokratis Karamitros, Gethsimani Papadopoulou, Maria Bousali, Anastasios Mexias, Sotirios Tsiodras, Andreas Mentis

SARS-CoV-2 exhibits intra-host genomic plasticity and low-frequency polymorphic quasispecies

Timokratis Karamitros[1#], Gethsimani Papadopoulou[1], Maria Bousali[1], Anastasios Mexias[1], Sotirios Tsiodras[2], Andreas Mentis[3]

1. Unit of Bioinformatics and Applied Genomics, Department of Microbiology, Hellenic Pasteur Institute, Athens, Greece
2. 4th Academic Department of Medicine, National and Kapodistrian University of Athens, Medical School, Athens, Greece.
3. Public Health Laboratories, Department of Microbiology, Hellenic Pasteur Institute, Athens, Greece

#To whom correspondence should be addressed:
Dr. Timokratis Karamitros
Researcher
Bioinformatics and Applied Genomics Unit
Department of Microbiology
Hellenic Pasteur Institute
127 Vas. Sophias avenue
11521, Athens, Greece
m: tkaram@pasteur.gr
t: +30 2106478-871, -874

ABSTRACT

In December 2019, an outbreak of atypical pneumonia (Coronavirus disease 2019 - COVID-19) associated with a novel coronavirus (SARS-CoV-2) was reported in Wuhan city, Hubei province, China. The outbreak was traced to a seafood wholesale market and human to human transmission was confirmed. The rapid spread and the death toll of the new epidemic warrants immediate intervention. The intra-host genomic variability of SARS-CoV-2 plays a pivotal role in the development of effective antiviral agents and vaccines, as well as in the design of accurate diagnostics.

We analyzed NGS data derived from clinical samples of three Chinese patients infected with SARS-CoV-2, in order to identify small- and large-scale intra-host variations in the viral genome. We identified tens of low- or higher- frequency single nucleotide variations (SNVs) with variable density across the viral genome, affecting 7 out of 10 protein-coding viral genes. The majority of these SNVs (72/104) corresponded to missense changes. The annotation of the identified SNVs but also of all currently circulating strain variations revealed colocalization of intra-host as well as strain specific SNVs with primers and probes currently used in molecular diagnostics assays. Moreover, we de-novo assembled the viral genome, in order to isolate and validate intra-host structural variations and recombination breakpoints. The bioinformatics analysis disclosed genomic rearrangements over poly-A / poly-U regions located in ORF1ab and spike (S) gene, including a potential recombination hot-spot within S gene.

Our results highlight the intra-host genomic diversity and plasticity of SARS-CoV-2, pointing out genomic regions that are prone to alterations. The isolated SNVs and genomic rearrangements reflect the intra-patient capacity of the polymorphic quasispecies, which may arise rapidly during the outbreak, allowing immunological escape of the virus, offering resistance to anti-viral drugs and affecting the sensitivity of the molecular diagnostics assays.

KEYWORDS

SARS-CoV-2, COVID-19 epidemic, intra-host variability, quasispecies, genomic rearrangements, molecular diagnostics

Highlights

- SARS-CoV-2 exhibits intra-host small- and large-scale genomic variability
- SNVs are collocalized with probes and primers used in molecular diagnostic assays
- SARS-CoV-2 Spike (S) gene host a potential recombination hot-spot

INTRODUCTION

Coronaviruses (CoVs), considered to be the largest group of viruses, belong to the *Nidovirales* order, *Coronaviridae* family and *Coronavirinae* subfamily, which is further subdivided into four genera, the alpha- and betacoronaviruses, which infect mammalian species and gamma- and deltacoronaviruses infecting mainly birds [1,2]. Small mammals (mice, dogs, cats) serve as reservoirs for Human Coronaviruses (HCoVs), with significant diversity seen in bats, which are considered to be primordial hosts of HCoVs [3].

Until 2002, minor consideration was given to HCoVs, as they were associated with mild-to-severe disease phenotypes in immunocompetent people [3–5]. In 2002, the beginning of severe acute respiratory syndrome (SARS) outbreak took place [6]. In 2005, after the discovery of SARS-CoV-related viruses in horseshoe bats (*Rhinolophus*), palm civets were suggested as intermediate hosts, and bats as primordial hosts of the virus [6,7]. In 2012, the emerging Middle East respiratory syndrome coronavirus (MERS-CoV) caused an outbreak in Saudi Arabia, which affected both camels and humans, with a high mortality rate of approximately 34,3% among humans [8]. MERS-CoV has zoonotic origins [9] and was transmitted to humans through direct contact with dromedary camels or indirect contact with contaminated meat or milk[10].

On December 31st – 2019, a novel Coronavirus (SARS-CoV-2) was first reported from the city of Wuhan, Hubei province in China, causing severe infection of the respiratory tract in humans, after the identification of a group of similar cases of patients with pneumonia of unknown etiology [11]. Similarly to SARS, epidemiological links between the majority of COVID-19 cases and Huanan South China Seafood Market, a live-animal market, have been reported. A total of 76,775 confirmed cases of “Coronavirus Disease 2019” (COVID-19) were reported up to February 21st 2020, from which 2,247 died and 18,855 recovered. Notably, 75,447 of the confirmed cases were reported in China [12].

The size of the ssRNA genome of SARS-CoV-2 is 29,891 nucleotides, it encodes 9860 amino acids and is characterized by nucleotide identity of ~ 89% with bat SARS-

related (SL) CoV-ZXC21 and bat-SL-CoVZC45. However, when compared to HCoVs, SARS-CoV-2 showed genetic similarity of ~ 80% with human SARS-CoVs BJ01 2003 and Tor2 [13] and and 50% with MERS-CoV [14,15]. CoVs are enveloped positive-sense RNA viruses, characterized by a very large non-segmented genome (26 to 32kb length), ready to be translated [2,4]. The genes arrangement on the SARS-CoV-2 genome is: 5′UTR -replicase (ORF1/ab) -Spike (S) -ORF3a -Envelope (E) -Membrane (M) -ORF6 -ORF7a -ORF8 -Nucleocapsid (N) ORF10 -3′UTR [13]. SARS-CoV-2 encodes proteins that are very similar in length compared to bat-SL-CoVZC45 and bat-SL-CoVZXC21. The SARS-CoV-2 S protein however is longer compared to those encoded by SARS-CoV, and MERS-CoV [15].

At inter-host level, adaptive mutations are essential for the newly emerging viruses in order to increase replication and facilitate onward transmission in the new hosts [16]. Particularly for MERS-CoV, SARS-CoV and SARS-CoV-2, the genetic diversity and frequent recombination events, lead to periodical emergence of new viruses capable of infecting a wide range of hosts [17]. Intra-host variability in viral infections, emerges from genomic phenomena taking place during error-prone replication, ending up to multiple circulating quasispecies of low or higher frequency [18]. These variants, in combination with the genetic profile of the host, can potentially influence the natural history of the infection, the viral phenotype, but also the sensitivity of molecular and serological diagnostics assays [19,20]. In the case of flu epidemics for example, de novo arising mutations and intra-host diversity not only forms intra-host evolution of Influenza A, but also greatly affects the pathogenesis of the virus [21–23]. Indeed, it is suggested that SARS-CoV-2 genomic variants that emerge from inter- and intra-host evolution might be associated with susceptibility to SARS-CoV-2 infection and the severity of COVID-19 [24].

Viruses have developed multiple adaptive strategies to counteract the host immunological response, which are subject to inter- and intra-host selection pressures; “Selfish” strategies confer a selective advantage in a particular quasispecies, impair the immune response inside the infected cell and evolve by intra-host selection, while neutral or “unselfish” defence strategies impair the immune response outside the infected cell and

evolve by inter-host selection, preferentially in viruses with low mutation rates [25]. SARS-CoV-2 mutation rate is moderate and similar to other RNA viruses (0.00084 per site per year) [26], but still generally higher compared to DNA viruses [27]. Moreover, most of the suggested immune escape mechanisms of SARS-CoV-2 involve intra-cellular interactions [28], thus expected to evolve by intra-host selective pressure. These observations highlight the importance of SARS-CoV-2 intra-host variability in the frame of viral evolution and host-pathogen interactions.

Intra-host genomic variability also leads to antigenic variability, which is of higher importance, especially for pathogens that fail to elicit long-lasting immunity in their hosts, and remains a major contributor to the complexity of vaccine design [29,30]. To date, there are no clinically approved vaccines available for protection of general population from SARS- and MERS-CoV infections as there is no effective vaccine to induce robust cell mediated and humoral immune responses [31,32].

Here, we explore intra-host genomic variants and low-frequency polymorphic quasispecies in Next Generation Sequencing (NGS) data derived from patients infected by SARS-CoV-2. Intra-host genomic variability is critical for the development of novel drugs and vaccines, which are of urgent necessity, towards the containment of the pandemic.

MATERIALS AND METHODS

In this study NGS data derived from three Chinese patients (oral swabs) infected by SARS-CoV-2 were analysed (SRA projects PRJNA601736 and PRJNA603194). All datasets available in SRA up to February 20th, 2020 were analysed. The two patients (SRR10903401 and SRR10903402/PRJNA601736), 39- and 21-year-old respectively, experienced unusual pneumonia. Despite his anti-viral treatment, patient 1 experienced more severe symptoms The two patients were admitted to the hospital on 25th and 22th December 2019 and were

discharged in stable condition on 12th and 11th January 2020, respectively [33]. The third 41-year-old male patient (SRR1097138/PRJNA603194), presented acute onset of common COVID19 symptoms. A combinatory antiviral therapy was administered to the patient. However, he exhibited respiratory failure and was admitted to the intensive care unit. Six days after his admission, he was transferred to another hospital in Wuhan for further treatment [34]. Detailed clinical metadata of the patients are presented in Supplementary Material.

The raw read data were aligned on the complete (29,891 bp) SARS-CoV-2 reference sequence (GenBank accession no. MN975262.1, isolate 2019-nCoV_HKU-SZ-005b_2020) using bowtie2 v2.3.0 [35], after quality check with FastQC v0.11.5 [36]. The resulting alignments were visualized with the *Integrated Genomics Viewer* (IGV) v2.3.60 [37]. After removing PCR duplicates, SNVs were called with a Bonferroni-corrected *P*-value threshold of 0.05 using *samtools* v1.7 (htslib1.7.2) [38] and *LoFreq* v2.1.5. LoFreq is a very accurate SNV caller especially designed for viral and bacterial genomes; its performance depends on the sequencing depth and the quality of the NGS reads. For the datasets analyzed in this study (average read depth 133.5x – 598.2x) and based on the assessed read quality >Q30 = 88.2 – 92.7%, LoFreq has calling sensitivity = ~1% and PPV=100 [39]. Variants supported by absolute read concordance (>98%) were filtered-out from intra-host variant frequency calculations. Four SNVs from sample SRR10903402 and 3 SNVs from sample SRR10971381 with statistically significant strand bias (*P*-value < 0.05) were also excluded from further analyses. Variations were annotated to the reference genome using snpEff v4.3p [40], SNVs effects were further filtered with snpSift v4.3p [41] and the average mutation rate per gene across the viral genome was estimated using R scripts (v3.6.2) in RStudio v1.1.456. The colocalization of the intra-host SNVs and population level SNPs retrieved from www.GISAID.org on February 18th 2020, with primers and probes coordinates was also examined, to identify potential interferences with all currently available molecular diagnostic assays [42]. The impact of these SNVs on the binding affinity of primers and probes to their genomic targets, was predicted using FastPCR 3.3.28 [43] and DINAMelt

webserver [44]. To investigate intra-host genomic rearrangements, *de novo* assembly of the SARS-CoV-2 genomes was performed using Spades v3.13.1 [45]. Spades outperforms most modern de novo assemblers in terms of viral genome retrieval and coverage, presenting the highest sensitivity (99.48%) [46]. The resulting contigs were analyzed with BLAST v2.6.0 [47] and confirmed by remapping of the raw reads, setting a threshold of 5 not replicated reads for contigs suggesting rearrangements. Smaller contigs (<200 bp) were elongated where possible, after pair-wise realignment of the corresponding mapped reads. Basic computations and visualizations were implemented in R programming language v3.6.2, using in-house scripts. The secondary structures of the genomic regions surrounding the recombination breakpoints were predicted using RNAfold webserver [48].

RESULTS

The mapping assembly of the viral genome was almost complete for all samples. The genome coverage and the average read depth across the genome was 100.0% and 133.5x for sample SRR10903401, 100.0% and 522.5x for sample SRR10903402, and 99.9%, and 598.2x for sample SRR10971381, respectively (**Table 1**).

In all samples, the same 5 SNVs isolated with 98-100% read concordance, thus in total divergence with the reference genome (MN975262.1), were excluded from downstream analysis. For sample SRR10903401 34 lower frequency SNVs were isolated in total. Of these, 33 were present with frequencies ranking between 2 and 15%, while only one was present in 40% of the intra-host viral population. The sequencing depth, which is also evaluated during the SNV calling by the LoFreq algorithm, ranked between 39x and 290x at the corresponding SNV positions. The sequencing depth of sample SRR10903402 at the polymorphic positions was higher (103x – 1137x), allowing the isolation of 55 SNVs with frequencies distributed between 0.9% and 14%. The depth over the polymorphic positions of

sample SRR10971381 was between 159x – 1872x, allowing the isolation of 10 intra-host SNVs, with frequencies 1.1% - 6.8% (**Figure 1.A, Suppl.Table 1**).

Intra-host variants were distributed across 7 out of the 10 protein-coding genes of the viral genome, namely ORF1ab, S, ORF3a, ORF6, ORF7a, ORF8 and N. After normalising for the gene length (variants/kb-gene-length, "v/kbgl"), the density of the SNVs for each gene was estimated (**Table 2**). The majority of the SNPs corresponded to missense changes (leading to amino-acid change) compared to synonymous changes (cumulatively 72 vs. 29 respectively, ratio 2.48:1) (**Table 2**), while the average number of missense changes was marginally significantly higher compared to synonymous changes (23,3 vs. 8,0 respectively, Wilcoxon rank sum test, $p=0.054$). The average intra-host variant frequency did not differ significantly either between missense and synonymous polymorphisms (Wilcoxon rank sum test, $p>0.05$) (**Figure 1.C**), or between their hosting genes (pairwise Wilcoxon rank sum tests, $p>0.05$) (**Figure 1.D**). We did not detect any small-scale insertions or deletions in the samples (**Suppl. Table 1**).

The comparison of all SNVs (intra-host and population level) with the genomic targets of the molecular diagnostics assays, revealed colocalization of 3 intra-host SNVs and 2 isolate-specific SNVs with primers and probes currently in use in RdRP_SARSr, HKU-N, 2019-nCoV-N1 and 2019-nCoV-N2 diagnostic reactions (**Figure 2**). The thermodynamic assessment of these SNVs revealed variable impact on the binding affinity of the corresponding primers and probes on the mutated genomic region (**Suppl. Table 2**)

The *de novo* assembly of the viral genomes was almost complete for samples SRR10903401 and SRR10903402 covering 99.7 % of the genome with 4 overlapping contigs and 99.5% of the genome with a single contig, respectively. The de novo assembly of sample SRR10971381 was complete, with one contig covering 100% of the genome. Alternative contigs revealed intra-host genomic rearrangements **(Figure 3, Table 3)**. For samples SRR10903401 and SRR10903402, these large-scale structural events were systematically observed over poly-A / poly-U-rich genomic regions, located in ORF1ab and S genes. All rearrangements were validated by remapping of the raw reads on the

corresponding *de novo* assembled contigs, setting a threshold of at least 5 supporting reads of high mapping quality (>40) in each case. For sample SRR10903401 three inversions/misassemblies in ORF1ab (**Suppl. Figure 1**) and one inversion/misassembly in S gene (**Figure 4-A**) were isolated. Notably, we were able to validate the same inversion in S gene for sample SRR10903402 as well (**Figure 4-B**). Apart from 2 inversions in ORF1ab supported by only 2 reads each (not passing the validation threshold), there were no further large-scale intra-host events observed for sample SRR10903402. Similarly, one inversion/misassembly in sample SRR10971381 that was supported by only one read was identified. The alignment coordinates of all rearrangement-supporting contigs with respect to the reference strain are presented in **Table 3**.

DISCUSSION

The rapid spread and the death toll of the new SARS-CoV-2 epidemic warrants the immediate identification / development of effective antiviral agents and vaccines, and the design of accurate diagnostics as well. The intra- and inter- patient variability affects the compatibility of molecular diagnostics but also impairs the effectiveness of the vaccines and the serological assays by altering the antigenicity of the virus.

All samples analysed in this study were probably infected by the same viral strain since they shared the same set of consensus SNVs. However, apart from 3 intra-host SNVs that were common between SRR10903401 and SRR10903402, there was no other overlap observed between the low frequency variants of each sample (**Figure 1-B**). This indicates that these variations have occurred in a rather random fashion and are not subject to selective pressures, which is also supported by the fact that the missense mutations were systematically more, compared to the synonymous mutations [49]. On the other hand, missense substitutions are more common in loci involving pathogen resistance, indicating positive selection [50]. The analysed viral RNA might have originated from functional/packed virions, but also from unpacked viral genomes, unable to replicate and infect other host cells. Even if a viral genome is unable to replicate independently, its abundant presence in the pool of viral quasispecies implies some functionality regarding the intra-host evolution and adaptation. For example, defective viral genomes might affect infection dynamics such as viral persistence as well as the natural history of the infection [51,52]. At the same time, these variants may arise rapidly during an outbreak and can be used for tracking the transmission chains and the spatiotemporal characteristics of the epidemic [53–55]. More studies based on genomic datasets accompanied by clinical metadata are needed, in order to accurately define associations between intra-host SARS-CoV-2 genomic variants, the progression and the clinical outcome of COVID19.

SNVs and quasispecies observed at low frequency could represent viral variations of low impact on the functionality of the genome. Bal et. al, suggest that development of quasispecies may promote viral evolution, however high depth of coverage is essential for the study of intra-host adaptation [56]. The abundance of low-frequency variations is largely affected by the population size and the epidemic characteristics. For example, a neutral substitution in a region that represents a primer target for a molecular diagnostic assay can drift to fixation rather quickly in a rapidly spreading virus, jeopardizing the sensitivity of the assay [57,58]. Here, we highlight three intra-host but also two fixed variants that are colocalized with primers or probes of real-time PCR diagnostics assays that are currently in use (**Figure 2**). Since the binding affinity of these oligos to their genomic targets (**Suppl.Table 2**) is directly linked to the performance of the corresponding diagnostic assays, the community should pay extra attention in the evaluation of these potentially emerging variations and be alerted, in case redesigning of these oligos is needed.

As it is well documented, recombination events lead to substantial changes in genetic diversity of RNA viruses [49,59]. In CoVs, discontinuous RNA synthesis is commonly observed, resulting in high frequencies of homologous recombination [60], which can be up to 25% across the entire CoV genome [61]. For pathogenic HCoVs genomic rearrangements are frequently reported during the course of epidemic outbreaks, such as HCoV-OC43 [62], and HCoV-NL63 [63], SARS-CoV [64][62] and MERS-CoV [65]. We have isolated intra-host genomic rearrangements, located in poly-A and poly-U enriched palindrome regions across the SARS-CoV-2 genome (**Figure 4**). We conclude that these rearrangements do not represent artifacts derived from the NGS library preparation (e.g. PCR crosstalk artifacts), especially since all the supporting reads were not duplicated and, in some cases, differed in polymorphic positions (**Suppl. Figure 1**).

Recombination processes involving S gene particularly, have been reported for SARS- and SARS-like CoV but also for HCoV-OC43. In the case of sister species HCoV-NL63 and HCoV-229E, recombination breakpoints are located near 3'- and 5'-end of the gene [1][65]. S is a trimeric protein, which is cleaved into two subunits, the globular N-

terminal S1 and the C-terminal S2 [66]. Our analysis revealed that similarly to other genomic regions, the S1 subunit hosts many low-frequency SNVs, characterized by higher density compared to the rest of the S gene sequence (**Figure 1-E**). The S2 subunit is highly conserved [13] and contains two fusion peptides (FP, IFP) [66]. In S gene, the same rearrangement event has taken place in two samples analyzed in this study, located in nt24,000, which corresponds to the ~200nt linking region between FP and IFP (aa 812-813). This observation highlights a potential recombination hot-spot. Examining closely the secondary structure of the RNA genome around the breakpoints, we suggest a model where the palindromes 5'-UGGUUUU-3' and 5'-AAAACCAA-3', have served as donor-acceptor sequences during the recombination event, since they are both exposed in the single-stranded internal loops formed in a highly structured RNA pseudoknot (**Figure 4-C**). The RB domain of the S protein has been tested as a potential immunogen as it contains neutralization epitopes which appear to have a role in the induction of neutralizing antibodies [31]. It should be mentioned though that the S protein of SARS-CoV is the most divergent in all strains infecting humans [67], as in both C and N-terminal domains variations arise rapidly, allowing immunological escape [68]. Our findings support that apart from these variations, the N-terminal region also hosts a recombination hot-spot, which together with the rest of the observed rearrangements, indicates the genomic instability of SARS-CoV-2 over poly-A and poly-U regions.

Authors' contributions: TK: Conceptualization; Data curation; Formal analysis; Methodology; Supervision; Validation; Visualization; Writing - original draft; Writing - review & editing. GP: Data curation; Formal analysis; Writing - original draft; Writing - review & editing. MB: Visualization; Writing - review & editing. AM, ST and AM: Writing - original draft; Writing - review & editing.

Ethics approval and consent to participate: Not applicable.

Declarations of interest: None.

This research did not receive any specific grant from funding agencies in the public, commercial, or not-for-profit sectors.

FIGURE LEGENTS

Figure 1: Intra – host SNVs: (A) Intra host SNV frequency vs sequencing read depth (X coverage) in the corresponding alignment position. (B) Venn diagram representing unique and common SNVs isolated from the three patients (C) Boxplot of intra-host SNVs frequency vs. SNV type – synonymous, missense, nonsense (stop gained) (low, moderate and high impact respectively). Average values are in red rhombs. (D) Intra-host SNVs frequency vs. all seven genes affected (ORF1ab, S, ORF3a, ORF6, ORF7a, ORF8, N). Average values are in red rhombs. (E) Density histogram of intra-host SNVs isolated from all patients (total number of SNVs / 100 bp - blue bars) and average sequencing read depth (X coverage – green line), across the SARS-CoV-2 genome map (genes in orange, 5' and 3' untranslated regions in light blue).

Figure 2: Truncated map of SARS-CoV-2 genome illustrating a subset of intra-host (blue lines) and globally collected, isolate-specific SNVs (orange lines) with respect to the genomic targets of molecular diagnostics assays (red arrows – primers, red bars - probes). Three intra-host variants (orange triangles), and two strain specific variants (Wuhan/IVD-HB-04/2020 and Chongqing/YC01/2020 - red triangles), are colocalized with the RdRP_SARSr probe (15,474 T > G), the 2019-nCoV_N1 forward primer (28,291 C > T), the HKU-N reverse primer (28,971 A > G) and the 2019-nCoV-N2 probe (29,188 T > C and 29,200 C > T).

Figure 3: Alignment of the de novo assembled contigs on the genomic map (bottom). Concordantly aligned contigs (correct or gapped) are in green, while discordantly aligned contigs are in red. Sequencing read depth (X coverage) across the genome (blue histograms) and relative % GC content (green line) is presented for each sample.

Figure 4: Recombination events in S gene. Samples (A) SRR10903401 and (B) SRR10903402. Alignments of the de novo assembled contigs with respect to the reference genome (MN 975262). Donor – acceptor palindrome sequences are indicated in green bars. Raw, non-duplicated NGS reads, validating the recombination event, are represented below the corresponding contig. (C): Prediction of the secondary structure of the genomic region spanning the rearrangement breakpoint (100 bases upstream and 100 bases downstream). The corresponding donor- acceptor sequences, exposed in internal loops, are indicated in green bars.

REFERENCES

[1] V.M. Corman, D. Muth, D. Niemeyer, C. Drosten, Hosts and Sources of Endemic Human Coronaviruses, 100 (2018) 163–188. https://doi.org/10.1016/bs.aivir.2018.01.001.

[2] A.R. Fehr, S. Perlman, HHS Public Access, (2016) 1–23. https://doi.org/10.1007/978-1-4939-2438-7.

[3] D. Vijaykrishna, G.J.D. Smith, J.X. Zhang, J.S.M. Peiris, H. Chen, Y. Guan, Evolutionary Insights into the Ecology of Coronaviruses, J. Virol. 81 (2007) 4012–4020. https://doi.org/10.1128/jvi.02605-06.

[4] F. Li, W. Li, M. Farzan, S.C. Harrison, Structural biology: Structure of SARS coronavirus spike receptor-binding domain complexed with receptor, Science (80-.). 309 (2005) 1864–1868. https://doi.org/10.1126/science.1116480.

[5] C.I. Paules, Coronavirus Infections — More Than Just the Common Cold, 2520 (2020) 3–4. https://doi.org/10.1007/82.

[6] J. Cui, Origin and evolution of pathogenic coronaviruses, Nat. Rev. Microbiol. 17 (2019) 181–192. https://doi.org/10.1038/s41579-018-0118-9.

[7] J.H. Epstein, J. McEachern, J. Zhang, P. Daszak, H. Wang, H. Field, W. Li, B.T. Eaton, L.-F. Wang, M. Yu, Z. Hu, S. Zhang, Z. Shi, G. Crameri, H. Zhang, W. Ren, C. Smith, Bats Are Natural Reservoirs of SARS-Like Coronaviruses, Science (80-.). 310 (2005) 676–679. https://doi.org/10.1109/NEMS.2006.334722.

[8] Z.A. Memish, S. Perlman, M.D. Van Kerkhove, A. Zumla, Middle East respiratory syndrome., Lancet (London, England). 395 (2020) 1063–1077. https://doi.org/10.1016/S0140-6736(19)33221-0.

[9] E. Prompetchara, C. Ketloy, T. Palaga, Immune responses in COVID-19 and potential vaccines: Lessons learned from SARS and MERS epidemic., Asian Pacific J. Allergy Immunol. 38 (2020) 1–9. https://doi.org/10.12932/AP-200220-0772.

[10] F.S. Aleanizy, N. Mohmed, F.Y. Alqahtani, R.A. El Hadi Mohamed, Outbreak of Middle East respiratory syndrome coronavirus in Saudi Arabia: a retrospective study, BMC Infect. Dis. 17 (2017) 23. https://doi.org/10.1186/s12879-016-2137-3.

[11] WHO | Pneumonia of unknown cause –www.who.int/csr/don/05-january-2020-pneumonia-of-unkown-cause-china/, (2020). https://www.who.int/csr/don/05-january-2020-pneumonia-of-unkown-cause-china/en/#.XyAbsvYF-rc.mendeley (accessed July 28, 2020).

[12] GISAID | www.gisaid.org/epiflu-applications/global-cases-betacov, (n.d.).

[13] J.F. Chan, K. Kok, Z. Zhu, H. Chu, K. Kai-wang, S. Yuan, K. Yuen, Genomic characterization of the 2019 novel human-pathogenic coronavirus isolated from a

patient with atypical pneumonia after visiting Wuhan, 1751 (2020). https://doi.org/10.1080/22221751.2020.1719902.

[14] A.A. Rabaan, S.H. Al-Ahmed, S. Haque, R. Sah, R. Tiwari, Y.S. Malik, K. Dhama, M.I. Yatoo, D.K. Bonilla-Aldana, A.J. Rodriguez-Morales, SARS-CoV-2, SARS-CoV, and MERS-COV: A comparative overview., Le Infez. Med. 28 (2020) 174–184.

[15] R. Lu, X. Zhao, J. Li, P. Niu, B. Yang, H. Wu, W. Wang, H. Song, B. Huang, N. Zhu, Y. Bi, X. Ma, F. Zhan, L. Wang, T. Hu, H. Zhou, Z. Hu, W. Zhou, L. Zhao, J. Chen, Y. Meng, J. Wang, Y. Lin, J. Yuan, Z. Xie, J. Ma, W.J. Liu, D. Wang, W. Xu, E.C. Holmes, G.F. Gao, G. Wu, W. Chen, W. Shi, W. Tan, Genomic characterisation and epidemiology of 2019 novel coronavirus: implications for virus origins and receptor binding., Lancet (London, England). 395 (2020) 565–574. https://doi.org/10.1016/S0140-6736(20)30251-8.

[16] R. Antia, R.R. Regoes, J.C. Koella, C.T. Bergstrom, The role of evolution in the emergence of infectious diseases, Nature. 426 (2003) 658–661. https://doi.org/10.1038/nature02104.

[17] C. TaŞtan, B. Yurtsever, G. Sir KarakuŞ, D. Dİlek KanÇaĞi, S. Demİr, S. Abanuz, U. Seyİs, M. Yildirim, R. Kuzay, Ö. Elİbol, S. Arbak, M. AÇikel Elmas, S. BİrdoĞan, O.U. Sezerman, A.S. KocagÖz, K. YalÇin, E. Ovali, SARS-CoV-2 isolation and propagation from Turkish COVID-19 patients, Turkish J. Biol. = Turk Biyol. Derg. 44 (2020) 192–202. https://doi.org/10.3906/biy-2004-113.

[18] A. Beloukas, E. Magiorkinis, G. Magiorkinis, A. Zavitsanou, T. Karamitros, A. Hatzakis, D. Paraskevis, Assessment of phylogenetic sensitivity for reconstructing HIV-1 epidemiological relationships, Virus Res. 166 (2012) 54–60.

[19] M. Vignuzzi, J.K. Stone, J.J. Arnold, C.E. Cameron, R. Andino, Quasispecies diversity determines pathogenesis through cooperative interactions in a viral population, Nature. 439 (2006) 344–348. https://doi.org/10.1038/nature04388.

[20] T. Karamitros, G. Papatheodoridis, E. Dimopoulou, M.-V. Papageorgiou, D. Paraskevis, G. Magiorkinis, V. Sypsa, A. Hatzakis, The interferon receptor-1 promoter polymorphisms affect the outcome of Caucasians with HB eAg-negative chronic HBV infection, Liver Int. 35 (2015) 2506–2513.

[21] K.S. Xue, L.H. Moncla, T. Bedford, J.D. Bloom, Within-Host Evolution of Human Influenza Virus, Trends Microbiol. 26 (2018) 781–793. https://doi.org/https://doi.org/10.1016/j.tim.2018.02.007.

[22] G. Destras, M. Pichon, B. Simon, M. Valette, V. Escuret, P.-A. Bolze, G. Dubernard, P. Gaucherand, B. Lina, L. Josset, Impact of Pregnancy on Intra-Host Genetic Diversity of Influenza A Viruses in Hospitalised Women: A Retrospective Cohort Study., J. Clin. Med. 9 (2019). https://doi.org/10.3390/jcm9010058.

[23] B. Simon, M. Pichon, M. Valette, G. Burfin, M. Richard, B. Lina, L. Josset, Whole Genome Sequencing of A(H3N2) Influenza Viruses Reveals Variants Associated with Severity during the 2016–2017 Season, Viruses. 11 (2019) 108. https://doi.org/10.3390/v11020108.

[24] Y. Toyoshima, K. Nemoto, S. Matsumoto, Y. Nakamura, K. Kiyotani, SARS-CoV-2 genomic variations associated with mortality rate of COVID-19, J. Hum. Genet. (2020). https://doi.org/10.1038/s10038-020-0808-9.

[25] S. Bonhoeffer, M.A. Nowak, Intra-host versus inter-host selection: viral strategies of immune function impairment, Proc. Natl. Acad. Sci. U. S. A. 91 (1994) 8062–8066. https://doi.org/10.1073/pnas.91.17.8062.

[26] T. Day, S. Gandon, S. Lion, S.P. Otto, On the evolutionary epidemiology of SARS-CoV-2, Curr. Biol. (2020). https://doi.org/https://doi.org/10.1016/j.cub.2020.06.031.

[27] E.C. Holmes, The comparative genomics of viral emergence, Proc. Natl. Acad. Sci. 107 (2010) 1742–1746. https://doi.org/10.1073/PNAS.0906193106.

[28] S. Kumar, R. Nyodu, V.K. Maurya, S.K. Saxena, Host Immune Response and Immunobiology of Human SARS-CoV-2 Infection, Coronavirus Dis. 2019 Epidemiol. Pathog. Diagnosis, Ther. (2020) 43–53. https://doi.org/10.1007/978-981-15-4814-7_5.

[29] R. Malley, K. Trzcinski, A. Srivastava, C.M. Thompson, P.W. Anderson, M. Lipsitch, CD4+ T cells mediate antibody-independent acquired immunity to pneumococcal colonization, Proc. Natl. Acad. Sci. U. S. A. 102 (2005) 4848–4853. https://doi.org/10.1073/pnas.0501254102.

[30] M. Lipsitch, J.J. O'Hagan, Patterns of antigenic diversity and the mechanisms that maintain them, J. R. Soc. Interface. 4 (2007) 787–802. https://doi.org/10.1098/rsif.2007.0229.

[31] C.Y. Yong, H.K. Ong, S.K. Yeap, K.L. Ho, W.S. Tan, Recent Advances in the Vaccine Development Against Middle East Respiratory Syndrome-Coronavirus, Front. Microbiol. 10 (2019) 1–18. https://doi.org/10.3389/fmicb.2019.01781.

[32] R.J. Nicolas W. Cortes-Penfield, Barbara W. Trautner, A decade after SARS: Strategies to control emerging coronaviruses, Physiol. Behav. 176 (2017) 139–148. https://doi.org/10.1016/j.physbeh.2017.03.040.

[33] L. Chen, W. Liu, Q. Zhang, K. Xu, G. Ye, W. Wu, Z. Sun, F. Liu, K. Wu, B. Zhong, Y. Mei, W. Zhang, Y. Chen, Y. Li, M. Shi, K. Lan, Y. Liu, RNA based mNGS approach identifies a novel human coronavirus from two individual pneumonia cases in 2019 Wuhan outbreak, Emerg. Microbes Infect. 9 (2020) 313–319. https://doi.org/10.1080/22221751.2020.1725399.

[34] F. Wu, S. Zhao, B. Yu, Y.-M. Chen, W. Wang, Z.-G. Song, Y. Hu, Z.-W. Tao, J.-H. Tian, Y.-Y. Pei, M.-L. Yuan, Y.-L. Zhang, F.-H. Dai, Y. Liu, Q.-M. Wang, J.-J. Zheng,

L. Xu, E.C. Holmes, Y.-Z. Zhang, A new coronavirus associated with human respiratory disease in China, Nature. 579 (2020) 265–269. https://doi.org/10.1038/s41586-020-2008-3.

[35] B. Langmead, S.L. Salzberg, Fast gapped-read alignment with Bowtie 2, Nat. Methods. 9 (2012) 357–359. https://doi.org/10.1038/nmeth.1923.

[36] S. Andrews, FastQC: A Quality Control Tool for High Throughput Sequence Data [Online]. Available online at: http://www.bioinformatics.babraham.ac.uk/projects/fastqc/, (2010).

[37] J.T. Robinson, H. Thorvaldsdóttir, A.M. Wenger, A. Zehir, J.P. Mesirov, Variant review with the integrative genomics viewer, Cancer Res. 77 (2017) e31–e34. https://doi.org/10.1158/0008-5472.CAN-17-0337.

[38] H. Li, B. Handsaker, A. Wysoker, T. Fennell, J. Ruan, N. Homer, G. Marth, G. Abecasis, R. Durbin, The Sequence Alignment/Map format and SAMtools, Bioinformatics. 25 (2009) 2078–2079. https://doi.org/10.1093/bioinformatics/btp352.

[39] A. Wilm, P.P.K. Aw, D. Bertrand, G.H.T. Yeo, S.H. Ong, C.H. Wong, C.C. Khor, R. Petric, M.L. Hibberd, N. Nagarajan, LoFreq: A sequence-quality aware, ultra-sensitive variant caller for uncovering cell-population heterogeneity from high-throughput sequencing datasets, Nucleic Acids Res. 40 (2012) 11189–11201. https://doi.org/10.1093/nar/gks918.

[40] P. Cingolani, A. Platts, L.L. Wang, M. Coon, T. Nguyen, L. Wang, S.J. Land, X. Lu, D.M. Ruden, A program for annotating and predicting the effects of single nucleotide polymorphisms, SnpEff: SNPs in the genome of Drosophila melanogaster strain w1118; iso-2; iso-3, Fly (Austin). 6 (2012) 80–92. https://doi.org/10.4161/fly.19695.

[41] P. Cingolani, V.M. Patel, M. Coon, T. Nguyen, S.J. Land, D.M. Ruden, X. Lu, Using Drosophila melanogaster as a model for genotoxic chemical mutational studies with a new program, SnpSift, Front. Genet. 3 (2012). https://doi.org/10.3389/fgene.2012.00035.

[42] V.M. Corman, O. Landt, M. Kaiser, R. Molenkamp, A. Meijer, D.K. Chu, T. Bleicker, S. Brünink, J. Schneider, M.L. Schmidt, D.G. Mulders, B.L. Haagmans, B. van der Veer, S. van den Brink, L. Wijsman, G. Goderski, J.L. Romette, J. Ellis, M. Zambon, M. Peiris, H. Goossens, C. Reusken, M.P. Koopmans, C. Drosten, Detection of 2019 novel coronavirus (2019-nCoV) by real-time RT-PCR, Euro Surveill. 25 (2020). https://doi.org/10.2807/1560-7917.ES.2020.25.3.2000045.

[43] R. Kalendar, B. Khassenov, Y. Ramankulov, O. Samuilova, K.I. Ivanov, FastPCR: An in silico tool for fast primer and probe design and advanced sequence analysis, Genomics. 109 (2017) 312–319. https://doi.org/https://doi.org/10.1016/j.ygeno.2017.05.005.

[44] N.R. Markham, M. Zuker, DINAMelt web server for nucleic acid melting prediction, Nucleic Acids Res. 33 (2005) W577–W581. https://doi.org/10.1093/nar/gki591.
[45] A. Bankevich, S. Nurk, D. Antipov, A.A. Gurevich, M. Dvorkin, A.S. Kulikov, V.M. Lesin, S.I. Nikolenko, S. Pham, A.D. Prjibelski, A. V. Pyshkin, A. V. Sirotkin, N. Vyahhi, G. Tesler, M.A. Alekseyev, P.A. Pevzner, SPAdes: A new genome assembly algorithm and its applications to single-cell sequencing, J. Comput. Biol. 19 (2012) 455–477. https://doi.org/10.1089/cmb.2012.0021.
[46] T.D.S. Sutton, A.G. Clooney, F.J. Ryan, R.P. Ross, C. Hill, Choice of assembly software has a critical impact on virome characterisation, Microbiome. 7 (2019) 12. https://doi.org/10.1186/s40168-019-0626-5.
[47] S.F. Altschul, W. Gish, W. Miller, E.W. Myers, D.J. Lipman, Basic local alignment search tool, J. Mol. Biol. 215 (1990) 403–410. https://doi.org/10.1016/S0022-2836(05)80360-2.
[48] A.R. Gruber, R. Lorenz, S.H. Bernhart, R. Neuböck, I.L. Hofacker, The Vienna RNA websuite., Nucleic Acids Res. 36 (2008) W70. https://doi.org/10.1093/nar/gkn188.
[49] E.-G. Kostaki, T. Karamitros, M. Bobkova, M. Oikonomopoulou, G. Magiorkinis, F. Garcia, A. Hatzakis, D. Paraskevis, Spatiotemporal characteristics of the HIV-1 CRF02_AG/CRF63_02A1 epidemic in Russia and Central Asia, AIDS Res. Hum. Retroviruses. 34 (2018) 415–420.
[50] D.N. Cooper, N.P. Group., Nature encyclopedia of the human genome, Nature Pub. Group, London; New York, 2003.
[51] J. Aaskov, K. Buzacott, H.M. Thu, K. Lowry, E.C. Holmes, Long-term transmission of defective RNA viruses in humans and Aedes mosquitoes, Science (80-.). 311 (2006) 236–238. https://doi.org/10.1126/science.1115030.
[52] E. Karamichali, H. Chihab, A. Kakkanas, A. Marchio, T. Karamitros, V. Pogka, A. Varaklioti, A. Kalliaropoulos, B. Martinez-Gonzales, P. Foka, others, HCV defective genomes promote persistent infection by modulating the viral life cycle, Front. Microbiol. 9 (2018) 2942.
[53] G. Magiorkinis, D. Paraskevis, O.-G. Pybus, T. Karamitros, T. Vasylyeva, M. Bobkova, A. Hatzakis, HIV-1 epidemic in Russia: an evolutionary epidemiology analysis, Lancet. 383 (2014) S71.
[54] D. Paraskevis, G.K. Nikolopoulos, V. Sypsa, M. Psichogiou, K. Pantavou, E. Kostaki, T. Karamitros, D. Paraskeva, J. Schneider, M. Malliori, others, Molecular investigation of HIV-1 cross-group transmissions during an outbreak among people who inject drugs (2011--2014) in Athens, Greece, Infect. Genet. Evol. 62 (2018) 11–16.
[55] G. Magiorkinis, T. Karamitros, T.I. Vasylyeva, L.D. Williams, J.L. Mbisa, A. Hatzakis, D. Paraskevis, S.R. Friedman, An innovative study design to assess the community

555 effect of interventions to mitigate HIV epidemics using transmission-chain
556 phylodynamics, Am. J. Epidemiol. 187 (2018) 2615–2622.
557 [56] A. Bal, G. Destras, A. Gaymard, M. Bouscambert-Duchamp, M. Valette, V. Escuret, E.
558 Frobert, G. Billaud, S. Trouillet-Assant, V. Cheynet, K. Brengel-Pesce, F. Morfin, B.
559 Lina, L. Josset, Molecular characterization of SARS-CoV-2 in the first COVID-19
560 cluster in France reveals an amino acid deletion in nsp2 (Asp268del), Clin. Microbiol.
561 Infect. 26 (2020) 960–962. https://doi.org/https://doi.org/10.1016/j.cmi.2020.03.020.
562 [57] J.Y. Noh, S.-W. Yoon, D.-J. Kim, M.-S. Lee, J.-H. Kim, W. Na, D. Song, D.G. Jeong,
563 H.K. Kim, Simultaneous detection of severe acute respiratory syndrome, Middle East
564 respiratory syndrome, and related bat coronaviruses by real-time reverse transcription
565 PCR., Arch. Virol. 162 (2017) 1617–1623. https://doi.org/10.1007/s00705-017-3281-9.
566 [58] T. Karamitros, D. Paraskevis, A. Hatzakis, M. Psichogiou, I. Elefsiniotis, T. Hurst, A.M.
567 Geretti, A. Beloukas, J. Frater, P. Klenerman, others, A contaminant-free assessment
568 of Endogenous Retroviral RNA in human plasma., Nat. Sci. Reports. 6 (2016) 33598.
569 [59] E.C. Holmes, The evolution and emergence of RNA viruses, Oxford University Press,
570 2009.
571 [60] M.M.C. Lai, RNA recombination in animal and plant viruses, Microbiol. Rev. 56 (1992)
572 61–79. https://doi.org/10.1128/mmbr.56.1.61-79.1992.
573 [61] R.S. Baric, K. Fu, M.C. Schaad, S.A. Stohlman, Establishing a genetic recombination
574 map for murine coronavirus strain A59 complementation groups, Virology. 177 (1990)
575 646–656. https://doi.org/10.1016/0042-6822(90)90530-5.
576 [62] S.K.P. Lau, P. Lee, A.K.L. Tsang, C.C.Y. Yip, H. Tse, R.A. Lee, L.-Y. So, Y.-L. Lau,
577 K.-H. Chan, P.C.Y. Woo, K.-Y. Yuen, Molecular Epidemiology of Human Coronavirus
578 OC43 Reveals Evolution of Different Genotypes over Time and Recent Emergence of
579 a Novel Genotype due to Natural Recombination, J. Virol. 85 (2011) 11325–11337.
580 https://doi.org/10.1128/jvi.05512-11.
581 [63] K. Pyrc, R. Dijkman, L. Deng, M.F. Jebbink, H.A. Ross, B. Berkhout, L. van der Hoek,
582 Mosaic Structure of Human Coronavirus NL63, One Thousand Years of Evolution, J.
583 Mol. Biol. 364 (2006) 964–973. https://doi.org/10.1016/j.jmb.2006.09.074.
584 [64] C.-C. Hon, T.-Y. Lam, Z.-L. Shi, A.J. Drummond, C.-W. Yip, F. Zeng, P.-Y. Lam, F.C.-
585 C. Leung, Evidence of the Recombinant Origin of a Bat Severe Acute Respiratory
586 Syndrome (SARS)-Like Coronavirus and Its Implications on the Direct Ancestor of
587 SARS Coronavirus, J. Virol. 82 (2008) 1819–1826. https://doi.org/10.1128/jvi.01926-
588 07.
589 [65] J.S.M. Sabir, T.T.Y. Lam, M.M.M. Ahmed, L. Li, Y. Shen, S.E.M. Abo-Aba, M.I.
590 Qureshi, M. Abu-Zeid, Y. Zhang, M.A. Khiyami, N.S. Alharbi, N.H. Hajrah, M.J. Sabir,
591 M.H.Z. Mutwakil, S.A. Kabli, F.A.S. Alsulaimany, A.Y. Obaid, B. Zhou, D.K. Smith,

E.C. Holmes, H. Zhu, Y. Guan, Co-circulation of three camel coronavirus species and recombination of MERS-CoVs in Saudi Arabia, Science (80-.). 351 (2016) 81–84. https://doi.org/10.1126/science.aac8608.

[66] G. Lu, Q. Wang, G.F. Gao, Bat-to-human: Spike features determining “host jump” of coronaviruses SARS-CoV, MERS-CoV, and beyond, Trends Microbiol. 23 (2015) 468–478. https://doi.org/10.1016/j.tim.2015.06.003.

[67] L. Enjuanes, M.L. DeDiego, E. Álvarez, D. Deming, T. Sheahan, R. Baric, Vaccines to prevent severe acute respiratory syndrome coronavirus-induced disease, Virus Res. 133 (2008) 45–62. https://doi.org/10.1016/j.virusres.2007.01.021.

[68] L. Jiaming, Y. Yanfeng, D. Yao, H. Yawei, B. Linlin, H. Baoying, Y. Jinghua, G.F. Gao, Q. Chuan, T. Wenjie, The recombinant N-terminal domain of spike proteins is a potential vaccine against Middle East respiratory syndrome coronavirus (MERS-CoV) infection, Vaccine. 35 (2017) 10–18. https://doi.org/10.1016/j.vaccine.2016.11.064.

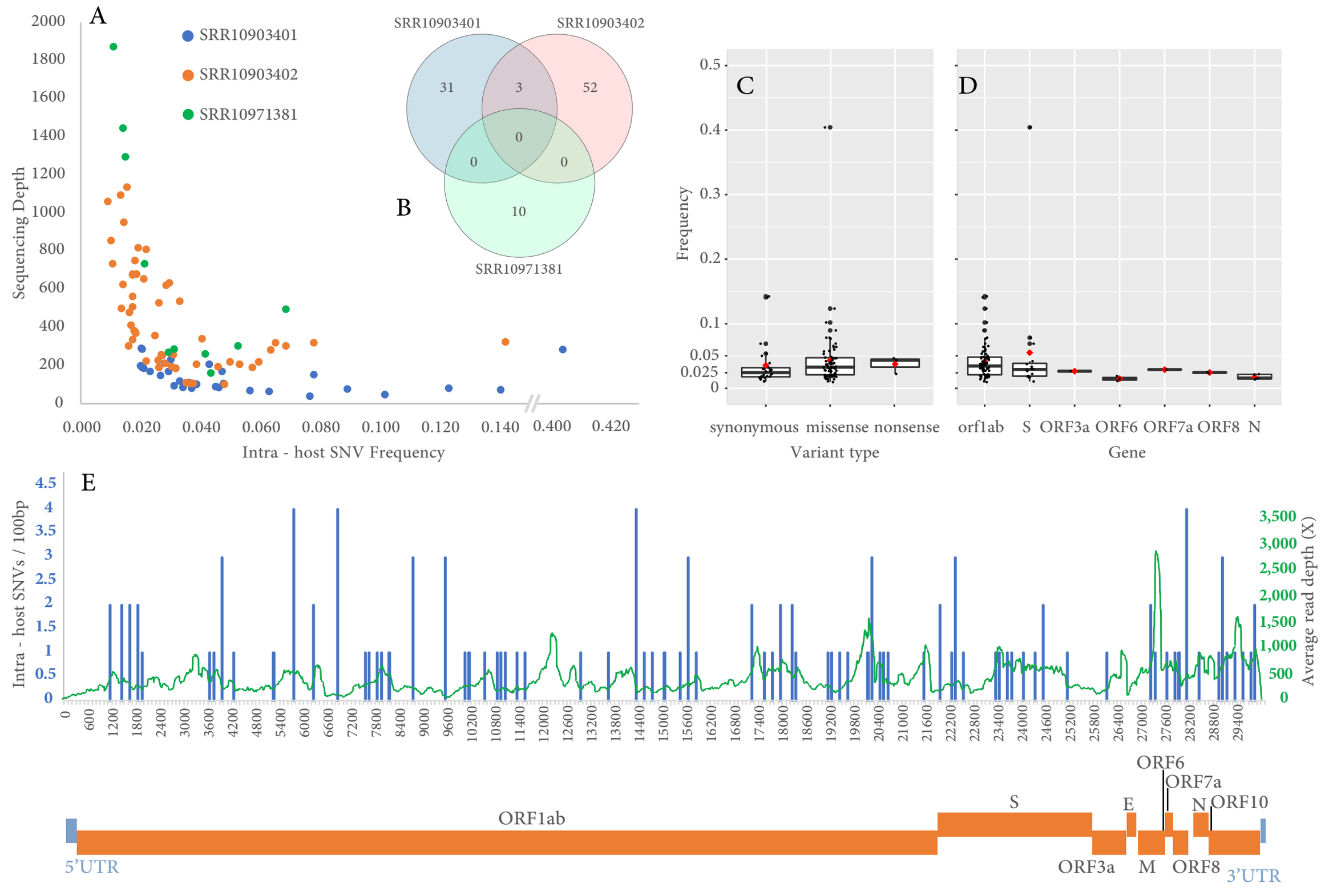
A
SRR10903401
SRR10903402
SRR10971381
Sequencing Depth
Intra - host SNV Frequency
B
SRR10903401
SRR10903402
SRR10971381
31
3
52
0
0
0
10
C
D
Frequency
synonymous
missense
nonsense
Variant type
orf1ab
S
ORF3a
ORF6
ORF7a
ORF8
N
Gene
E
Intra - host SNVs / 100bp
Average read depth (X)
ORF1ab
S
E
M
N
ORF3a
ORF6
ORF7a
ORF8
ORF10
5'UTR
3'UTR

1 100 200 300 400 500 600 700 800 900 1,000 1,100 1,200 1,300 1,400 1,500 1,600 1,700 1,800

global SNVs

intra-host SNVs

MN975262 — 5'UTR — orf1ab gene

13,100 13,200 13,300 13,400 13,500 13,600 13,700 13,800 13,900 14,000 14,100 14,200 14,300 14,400 14,500 14,600 14,700 14,800 14,900

global SNVs

intra-host SNVs

MN975262 — orf1ab gene

HKU-ORF1b-nsp14

15,000 15,100 15,200 15,300 15,400 15,500 15,600 15,700 15,800 15,900 16,000 16,100 16,200 16,300 16,400 16,500 16,600 16,700 16,800

global SNVs

intra-host SNVs

MN975262 — orf1ab gene

RdRP_SARSr

24,300 24,400 24,500 24,600 24,700 24,800 24,900 25,000 25,100 25,200 25,300 25,400 25,500 25,600 25,700 25,800 25,900 26,000 26,100

global SNVs

intra-host SNVs

MN975262 — S gene — ORF3a gene

26,200 26,300 26,400 26,500 26,600 26,700 26,800 26,900 27,000 27,100 27,200 27,300 27,400 27,500 27,600 27,700 27,800 27,900 28,000

global SNVs

intra-host SNVs

MN975262 — E gene — M gene — ORF6 gene — ORF7a gene — ORF8 ge...

E_Sarbeco

Wuhan/IVDC-HB-04/2020

Chongqing/YC01/2020

28,100 28,200 28,300 28,400 28,500 28,600 28,700 28,800 28,900 29,000 29,100 29,200 29,300 29,400 29,500 29,600 29,700 29,800 29,89

global SNVs

intra-host SNVs

MN975262 — ORF8 gene — N gene — N gene — ORF10 g... — 3'UTR

2019-nCoV-N1

2019-nCoV-N3

N_Sarbeco

HKU-N

2019-nCoV-N2

SRR10903401

Contigs aligned to MN975262.1

contig 6

contig 8

contig 7

contig 5

contig 3,4

contig 1

contig 2

0 2.99 5.98 8.97 11.96 14.95 17.93 20.92 23.91 26.9 29.89 kbp

Cov

300x

200x

100x

GC

80%

60%

40%

20%

SRR10903402

contig 2

contig 3

contig 4

contig 1

0 2.99 5.98 8.97 11.96 14.95 17.93 20.92 23.91 26.9 29.89 kbp

Cov

1500x

1000x

500x

GC

80%

60%

40%

20%

SRR10971381

contig 2

contig 1

0 2.99 5.98 8.97 11.96 14.95 17.93 20.92 23.91 26.9 29.89 kbp

2000x

1500x

1000x

500x

GC

80%

60%

40%

20%

ORF6

ORF7a

S

E

N

ORF10

ORF1ab

ORF3a

M

ORF8

5'UTR

3'UTR

0 2.99 5.98 8.97 11.96 14.95 17.93 20.92 23.91 26.9 29.89 kbp

A

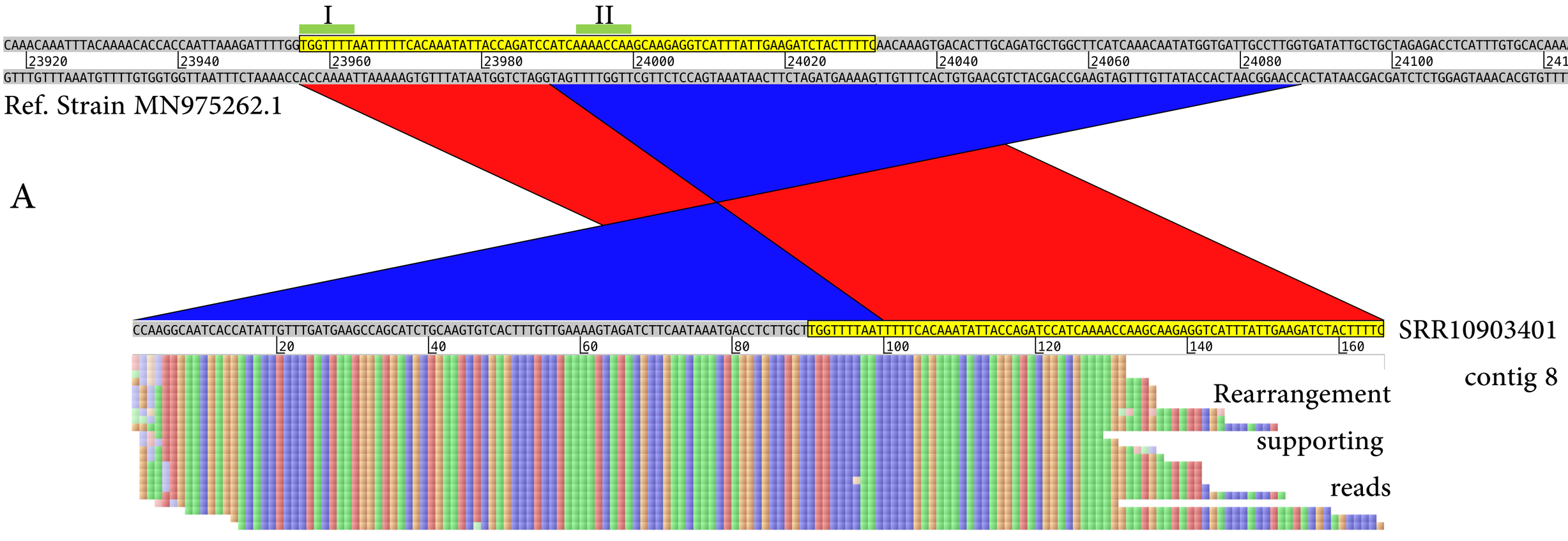
I
II
CAAACAAATTTACAAAACACCACCAATTAAAGATTTTGGTGGTTTTAATTTTTCACAAATATTACCAGATCCATCAAAACCAAGCAAGAGGTCATTTATTGAAGATCTACTTTTCAACAAAGTGACACTTGCAGATGCTGGCTTCATCAAACAATATGGTGATTGCCTTGGTGATATTGCTGCTAGAGACCTCATTTGTGCACAAAAGT
23920 23940 23960 23980 24000 24020 24040 24060 24080 24100 24120
GTTTGTTTAAATGTTTTGTGGTGGTTAATTTCTAAAACCACCAAAATTAAAAAGTGTTTATAATGGTCTAGGTAGTTTTGGTTCGTTCTCCAGTAAATAACTTCTAGATGAAAAGTTGTTTCACTGTGAACGTCTACGACCGAAGTAGTTTGTTATACCACTAACGGAACCACTATAACGACGATCTCTGGAGTAAACACGTGTTTTCA
Ref. Strain MN975262.1
CCAAGGCAATCACCATATTGTTTGATGAAGCCAGCATCTGCAAGTGTCACTTTGTTGAAAAGTAGATCTTCAATAAATGACCTCTTGCTTGGTTTTAATTTTTCACAAATATTACCAGATCCATCAAAACCAAGCAAGAGGTCATTTATTGAAGATCTACTTTTC
20 40 60 80 100 120 140 160
SRR10903401
contig 8
Rearrangement supporting reads

B

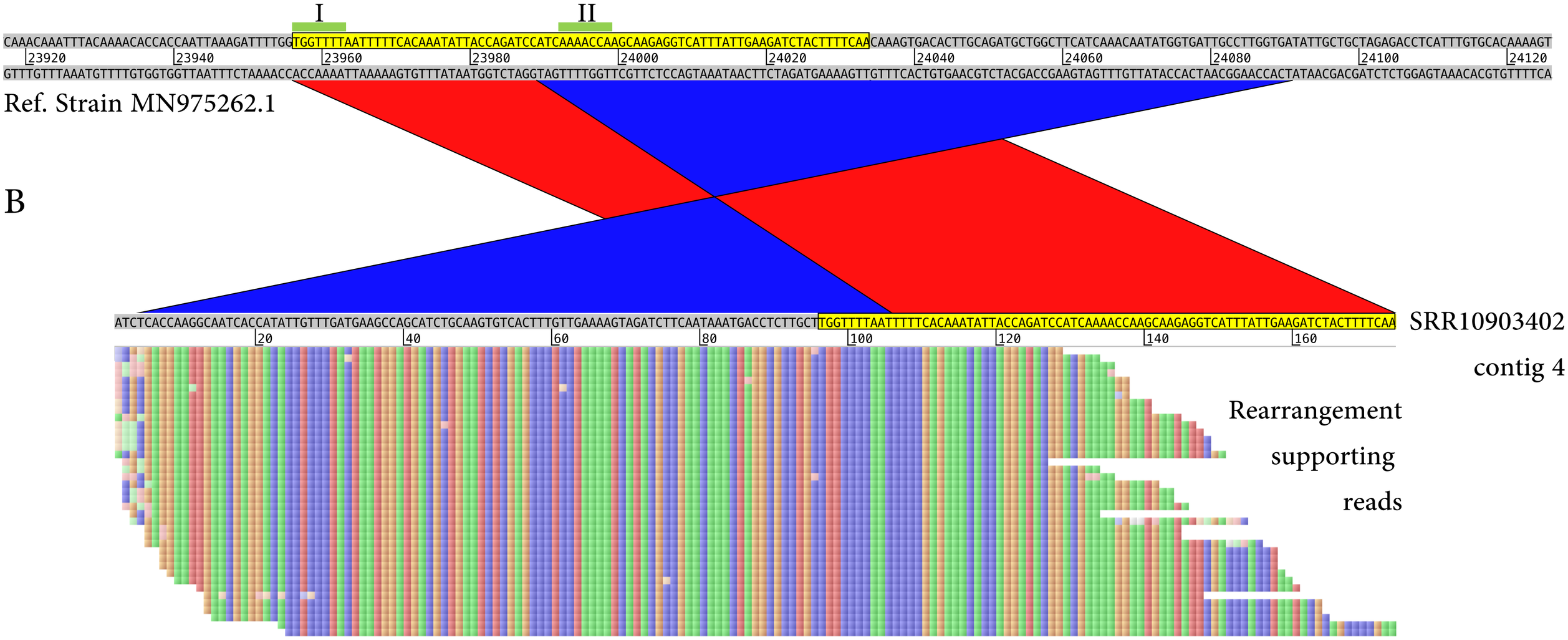
I
II
CAAACAAATTTACAAAACACCACCAATTAAAGATTTTGGTGGTTTTAATTTTTCACAAATATTACCAGATCCATCAAAACCAAGCAAGAGGTCATTTATTGAAGATCTACTTTTCAACAAAGTGACACTTGCAGATGCTGGCTTCATCAAACAATATGGTGATTGCCTTGGTGATATTGCTGCTAGAGACCTCATTTGTGCACAAAAGT
23920 23940 23960 23980 24000 24020 24040 24060 24080 24100 24120
GTTTGTTTAAATGTTTTGTGGTGGTTAATTTCTAAAACCACCAAAATTAAAAAGTGTTTATAATGGTCTAGGTAGTTTTGGTTCGTTCTCCAGTAAATAACTTCTAGATGAAAAGTTGTTTCACTGTGAACGTCTACGACCGAAGTAGTTTGTTATACCACTAACGGAACCACTATAACGACGATCTCTGGAGTAAACACGTGTTTTCA
Ref. Strain MN975262.1
ATCTCACCAAGGCAATCACCATATTGTTTGATGAAGCCAGCATCTGCAAGTGTCACTTTGTTGAAAAGTAGATCTTCAATAAATGACCTCTTGCTTGGTTTTAATTTTTCACAAATATTACCAGATCCATCAAAACCAAGCAAGAGGTCATTTATTGAAGATCTACTTTTCAA
20 40 60 80 100 120 140 160
SRR10903402
contig 4
Rearrangement supporting reads

C

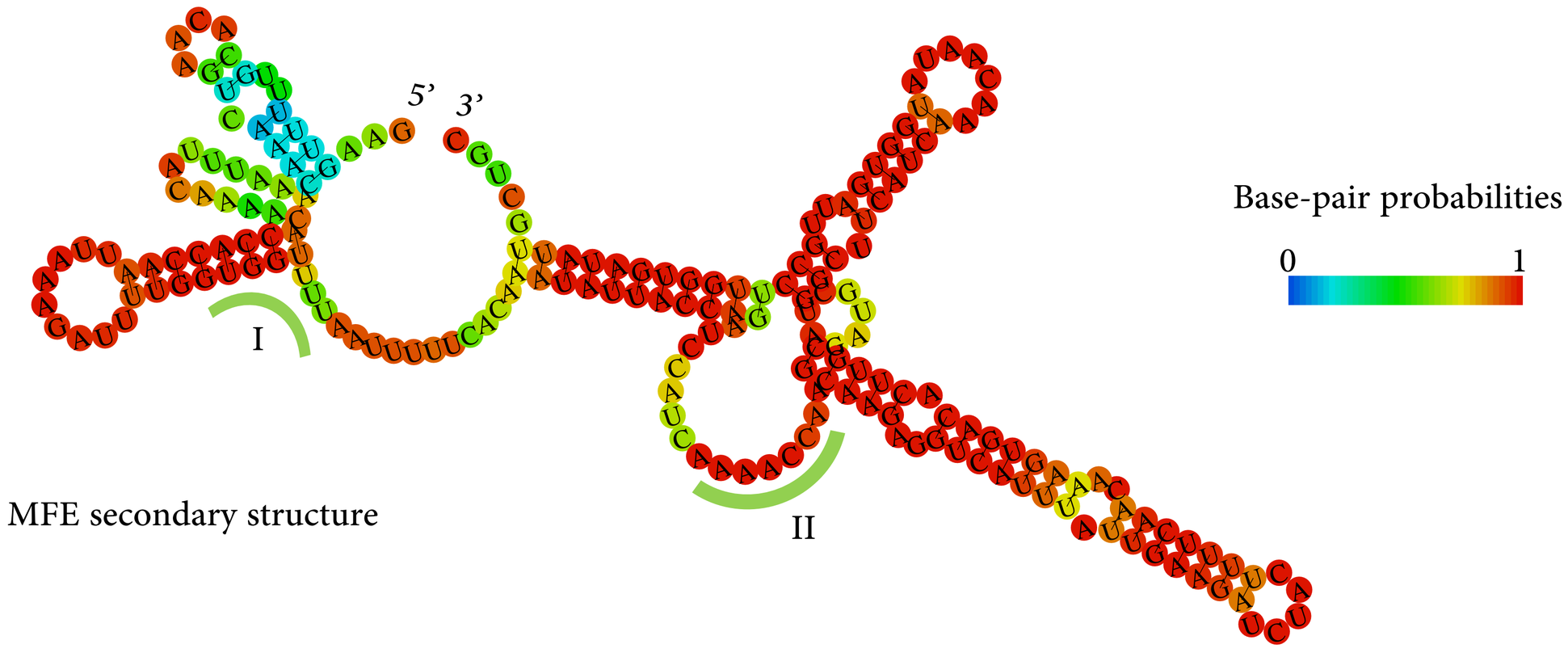
5’
3’
I
II
MFE secondary structure
Base-pair probabilities
0
1

TABLES

Table 1: NGS read alignment and genome coverage metrics

	Sample		
	SRR10903401	SRR10903402	SRR10971381
Paired Reads, N (%)			
Total Number	476632 (100)	676694 (100)	28282964 (100)
Aligned	13913 (2.94)	54723 (8.18)	62,288 (0.22)
Concordantly Aligned	11469 (2.40)	44176 (6.52)	59261(0.21)
Discordantly Aligned	2444 (0.53)	10547 (1.67)	3027 (0.01)
Single Mates, N (%)			
Aligned	244 (0.03)	1308 (0.11)	294(0.001)
Overall Alignment Rate (%)	2.94	8.18	0.22
Quality score >Q30 (%)	92.7	92.1	88.2
Genome Coverage (%)	100.0	100.0	99.9
Average read depth (X)	133.5	522.2	598.2

Table 2: Impact of Intra-host SNVs on viral genes

	Intra-host Variants Impact, N			
Gene	Low (synonymous)	Moderate (missense)	High (stop gained)	Total, N (v/kbgl)*
ORF1ab	19	53	2	74 (3.47)
S	6	9	1	16 (4.18)
ORF3a	0	1	0	1 (1.20)
E	0	0	0	0 (0)
M	0	0	0	0 (0)
ORF6	2	1	0	3 (16.21)
ORF7a	0	1	0	1 (2.73)
ORF8	0	3	0	3 (8.21)
N	2	4	0	6 (4.76)
ORF10	0	0	0	0 (0)
Total, N	29	72	3	

* normalised variants per 1 kb gene length (variants / gene-length *1000)

Table 3: Alignment characteristics of de novo assembled contigs

Contig Name	Contig Length	Reference* Coordinates		Contig Coordinates		Alignment Identity (%)	Alignment Type	Average Read Depth (x)	QC Pass#
		start	end	start	end				
SRR10903401 (99.7% coverage)									
Contig 1	23994	75	24068	23994	1	99.99	Correct	57.01	+
Contig 2	5681	24246	29891	1	5646	99.96	Correct	71.40	+
Contig 3	331	23992	24322	331	1	100	Correct	164.39	+
Contig 4	179	24221	24399	179	1	100	Correct	97.56	+
Contig 5	192	17816	17909	94	1	100	Inversion	7.22	+
		17933	18030	95	192	100	Correct		
Contig 6	181	18052	18152	101	1	100	Relocation, Inconsistency	8.12	+
		17766	17845	102	181	100	Misassembly		
Contig 7	169	1707	1765	62	4	100	Inversion	7.62	+
		1815	1903	63	151	97.75	Correct		
Contig 8	165	23992	24087	96	1	100	Inversion	18.04	+
		23963	24031	97	165	100	misassembly		
SRR10903402 (99.5% coverage)									
Contig 1	29842	133	29891	29842	84	99.98	Correct	234.32	+
Contig 2	242	2075	2139	178	242	100	Partial	1.09	-
Contig 3	242	21577	21629	242	190	100	Partial	1.06	-
Contig 4	173	23992	24090	102	4	100	Inversion	39.30	+
		23963	24033	103	173	100	Misassembly		
SRR10971381 (100.0% coverage)									
Contig 1	29902	1	29891	29897	7	99.98	Correct	267.59	+
Contig 2	241	516	559	163	120	100	Inversion	1.00	-
		472	501	119	90	100	Misassembly		

* Corresponding to reference MN975262 coordinates

contig supported by at least 5 non duplicated reads of mapping quality >40